

Analysis of the regimes in the scanner-based laser hardening process

S. Martínez^a, A. Lamikiz^{a*}, E. Ukar^a, A. Calleja^a, J.A. Arrizubieta^{a,b}, L.N. Lopez de Lacalle^a

^a Mechanical Engineering Dept. of University of the Basque Country UPV/EHU, Alameda Urquijo s/n, 48013 Bilbao, Spain

^b "La Caixa" Foundation Scholarship holder.

Corresponding author

Aitzol Lamikiz
Department of Mechanical Engineering, University of the Basque Country
ETSII-UPV, c/Alameda de Urquijo s/n, 48013 Bilbao, Spain
Tel: +34-946014221, Fax: +34-946014215
E-mail: aitzol.lamikiz@ehu.eus

Figures included in body text for easier review

Abstract:

Laser hardening is becoming a consolidated process in different industrial sectors such as the automotive industry or in the die and mold industry. The key to ensure the success in this process is to control the surface temperature and the hardened layer thickness. Furthermore, the development of reliable scanners, based on moving optics for guiding high power lasers at extremely fast speeds allows the rapid motion of laser spots, resulting on tailored shapes of swept areas by the laser. If a scanner is used to sweep a determined area, the laser energy density distribution can be adapted by varying parameters such as the scanning speed or laser power inside this area. Despite its advantages in terms of versatility, the use of scanners for the laser hardening process has not yet been introduced in the thermal hardening industry because of the difficulty of the temperature control and possible non-homogeneous hardness thickness layers.

In the present work the laser hardening process with scanning optics applied to AISI 1045 steel has been studied, with special emphasis on the influence of the scanning speed and the results derived from its variation, the evolution of the hardened layer thickness and different strategies for the control of the process temperature. For this purpose, the hardened material has been studied by measuring microhardness at different points and the shape of the hardened layer has also been evaluated. All tests have been performed using an experimental setup designed to keep a nominal temperature value using a closed-loop control. The tests results show two different regimes depending on the scanning speed and feed rate values. The experimental results conclusions have been validated by means of thermal simulations at different conditions.

Keywords: Laser hardening, scanner, surface treatment, AISI 1045

1. Introduction

Laser hardening is a surface hardening treatment used in different sectors such as the automotive industry or in the die and mold sector. The main benefits of the laser hardening technology, compared to more traditional hardening processes such as induction or flame hardening processes, are the higher performance in 3D complex shapes with a minimum heat affected zone and much lower thermal distortions. As a consequence of these advantages, in some cases, it is possible to reduce or even eliminate final finishing operations [1]. In addition, the interest of this process lies in the possibility of direct integration of a laser heat source on the production line without an additional quenching medium, as

well as the possibility to produce different microstructures in the part with a very accurate control between the treated and non-treated areas, resulting on a soft core with a hardened surface layer with compressive residual stresses in the surface [2]. This process is being used in the industry mainly for hardening stamping dies and molds. In particular, laser hardening is applied on the cutting edges of stamping dies, where it is possible to obtain a high surface hardness after the polishing operation with minimal geometric distortion. Laser hardening process is also being used in serial production of automotive components such as door hinges [1].

Laser hardening process can be considered a high speed surface treatment if it is compared with induction or flame hardening processes. Therefore, due to the high temperature gradients, the hardened layer thickness is usually between 0.8 and 1.5 mm, whereas conventional hardening process can reach values between 10-15mm. This is because the thickness of material that reaches the austenitization temperature (T_{AC3}) is lower than in conventional hardening processes.

Furthermore, in recent years a series of systems based on moving optics and traditionally applied for laser marking operations, are being used for guiding high power lasers. These systems are also called scanners and they can be coupled to the wrist of a serial robot [3] or in the spindle of a machine tool [4] in order to obtain a higher work-space. The main characteristic of the scanners is the ability to move and guide the laser beam with very high speeds (above 10,000 mm/s). The agility of the movements is obtained by the rotation of two mirrors, with very low mass and inertia.

The main advantages of scanners are the high processing speed and the working distance, which usually can be higher than 200 mm, and allows working far from the area to be processed. Currently, there are several research papers dedicated to the use of scanners in different manufacturing processes, particularly in the automotive industry such as marking, remote cutting or laser remote welding. Gradually these systems are being introduced in other industrial sectors such as the die and mold manufacturing industry where laser remote processes are being applied for texturing [5], polishing [6], drilling [7] or selective laser melting [8]. In contrast, the development of laser treatment processes based on scanning optics, also known as remote treatment processes, is still on a preliminary stage [9,10]. The main objective of this process is to move a laser beam rapidly, shaping the laser beam and obtaining a virtual shape (usually a line). With a conventional kinematics (Robot or Serial kinematics) the scanned shape is moved continuously on the hardened area. The main benefit of this variant is the possibility of adapting the size of the treated area at each point, unlike conventional laser hardening in which fixed optics with constant line widths are used. In the Fig. 1 a 2D scanner scheme and the laser hardening scanning strategy is shown.

Some researchers have been performed experimental tests in order to evaluate the process capabilities [11, 12, 13]. These works present different results about the feasibility of the process, and all agree on the importance of the process parameter control. One of the most relevant aspects on laser surface hardening is the in-process temperature control requirement. The temperature of the surface must be continuously verified during the whole process in order to avoid surface melting while maintaining the temperature higher than T_{AC3} . In addition, the temperature control becomes much more difficult in the scanner-based laser hardening process since the beam moves rapidly. Therefore, the set-up of the temperature control loop is one of the most challenging aspects on the laser surface hardening process with scanning optics.

In conventional laser hardening the laser beam dimensions define the width of the area to be hardened, without any possibility of modification. Specific optics are designed to distribute the power density in the most appropriate way inside the beam. These optics, made individually by diamond turning, are unique and high cost parts, where a fixed laser beam size and shape is obtained [14]. On the other hand, laser hardening with scanning optics use a software-based control to change the width of the hardened zone. Therefore, the main advantage introduced by the laser hardening process with scanner optics is the geometrical flexibility. The use of scanning optics allows adapting the distribution of the laser energy density in a determined area by changing the laser trajectory and by varying parameters such as the scanning speed and/or laser power inside this area. By contrast, the main disadvantage presented by the scanning optics in laser hardening process can be the non-homogeneous transformations because of excessive working speed of the laser and temperature variations due to the scanning strategy. In an extreme situation, there is the possibility of not achieving the minimum temperature for the transformation or, if the energy density is too high, cause the partial fusion of the treated area.

One of the main parameters to obtain homogeneous transformations in laser hardening process is the energy density, which must be set to obtain the required hardened layer depth but without reaching the melting point at any point on the source. Therefore, the main objective is to find the best combination of parameters to keep the process temperature

above the austenitization temperature as long as possible and improve the depth of hardened layer, without reaching the melting temperature at any point.

As it can be observed in Fig. 1b), laser hardening with scanning optics process presents two different speeds, the scanning speed and the feed rate (which is 600-1,000 times slower). One of the most characteristic parameters of this process is the scanning speed (V_S). It represents the guiding speed of the laser beam and it is controlled by the mirrors of the scanner, so the speed can reach up to 10,000 mm/s. On the other hand, the feed rate (V_F), which is the travel speed motion of the robot or machine tool, represents the speed of the hardened track on the part. During the scanning of the area to be hardened, while the machine moves to feed rate speed, the laser sweeps an area by moving the laser beam much faster. In Fig. 1b) the continuous scanning strategy is shown as well as the thermal field generated in a point on the surface, [15]. As it can be observed, the thermal field presents an inherent variation due to the scanning strategy. Therefore, the variation of the temperature could lead on non-homogeneous transformations.

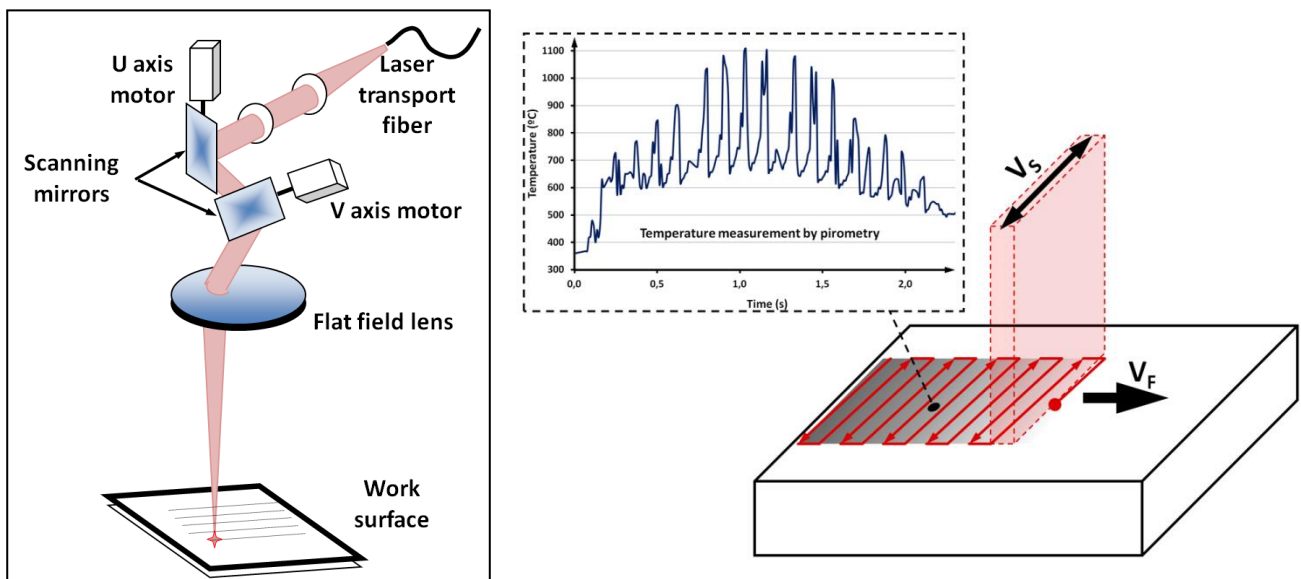


Fig. 1 a) A 2D scanner components; b) Continuous scanning strategy and thermal field generated in a point on the surface

Thus, in the present work, the strategies and parameters of laser hardening process with scanning optics will be studied, with special emphasis on the influence of the scanning speed and the results derived from its variation. The experimental tests have been focused on an AISI 1045 steel and different results have been measured such as microhardness, the shape and dimensions of the hardened layer and the loss of hardness in the overlapped areas between different scanned paths, since the main problem of overlapping paths in laser hardening process is the partial softening of these zones [16, 17]. All tests have been performed using a system that allows set a nominal temperature value using a temperature closed-loop control. Finally, the experimental conclusions will be verified by means of thermal simulations.

2. Experimental procedure

The laser hardening tests have been performed in a specially designed machine tool for laser material processing testing. The system is based on a converted 5 axes machining center with a 700x400x600 mm³ XYZ workspace and two rotary axes, B and C. The spindle has been replaced by a 2D scanner that can scan an area of 120x120 mm², which adds two additional linear axes, U and V. The laser system is a solid state fiber laser Rofin – Sinar FL010 with a maximum power of 1 KW, coupled to a 100 μm fiber connected to the scanner. Therefore, the system combines 7 axes: 5 axes of the machine (3 linear and 2 rotary), which can be considered as slow and long axes, and the two axes of the scanner, much faster and shorter. Thus, during the experimentation, the motion associated with the feed rate has been made with the machine axes and the ones associated with the scanning speed with the 2D scanner axes.

The laser power ranges from 100 W up to 1,000 W. considering the spot size obtained with the 100 microns fiber, the power density ranges between 1.27×10^6 W/cm² up to 1.27×10^7 W/cm². These power densities are too high for laser hardening process, since 10^4 - 10^5 W/cm² are used in fixed optics laser hardening process. Therefore, to perform the scanner-based laser hardening tests, the working area has been changed to obtain lower density powers. In particular, the beam has been defocused 50 mm in Z axis, resulting on a 1.2 mm diameter beam which, combined with high scanning speeds, result on two beneficial effects: First, the energy density is reduced because of the high speed and large beam diameter. On the other hand, higher working areas can be obtained by moving the laser faster. The change of the focal plane of the scanner, introduces a geometric error in the trajectory, which has to be also considered [18]. This error has been measured and compensated in the experimental tests. The complete experimental setup is shown in the Fig. 2.

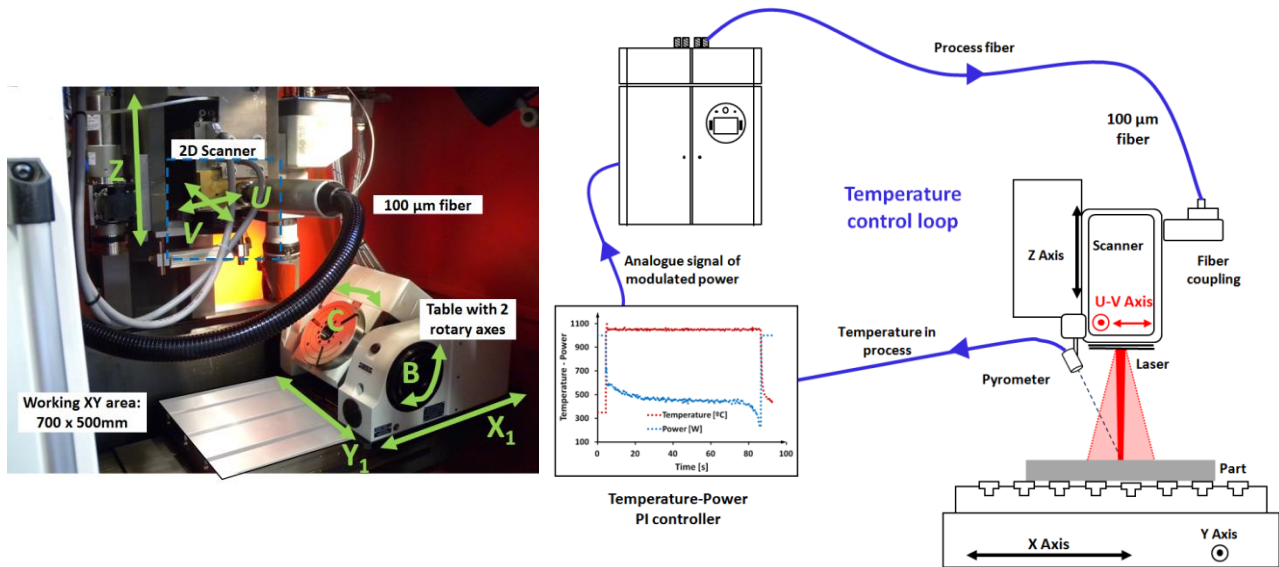


Fig. 2 a) Axes configuration of the laser machining center used for the experiments.; **b)** Temperature control in close-loop setup used during the experiments.

On the other hand, Fig. 2b) shows the temperature control setup used during the experimental tests. The system is based on a two color pyrometer that measures the temperature in the center of the track that is being hardened. Measured temperature is used as input value of a proportional-integral controller that adjusts the power signal each 50 ms to keep the nominal temperature during the process. The complete tuning of the PID control loop is described in [19]. In the Fig. 3a) both the actual temperature and the laser power are shown. As it can be observed, the variation of the power given by the control keeps a constant temperature nominal value of 1,050 °C. It can be observed that a higher power at the beginning is needed. Once the temperature is achieved, an almost constant power in the intermediate zone of the track is applied and, finally, a decrease of the laser power in the exit of the part is observed. These measurements are performed by positioning the pyrometer always in the hottest zone of the hardened area, corresponding to the center of the track that is being scanned.

During the laser hardening process with scanning optics, the thermal history of any point of the hardened area has two well differentiated zones that can be observed in the Fig. 3b): A background temperature and a maximum or peak temperature. To obtain this type of charts, the pyrometer has been placed on a fixed point of the scanned path. Thus, the temperature peaks are produced because of the effect of the zigzag scanning on the surface. As it can be observed, the result is an oscillating temperature which must be controlled to avoid damage or melted points on the part surface. Furthermore, the background temperature represents a more homogeneous and continuous heating of the part due to the thermal inertia of the part. According to the experimental results, the depth of the hardened layer depends mainly on the value of the background temperature during the process.

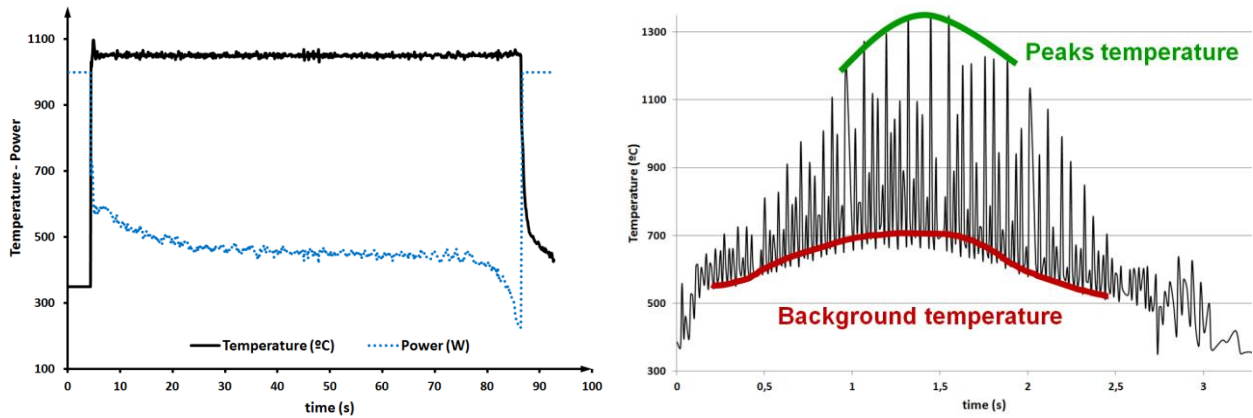


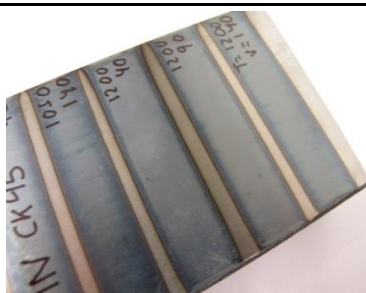
Fig. 3 a) Temperature and laser power evolution during a test; b) Evolution of the temperature at a fixed point on the surface of the part where the background temperature and the peaks temperatures are shown.

The longer is the threatened area above the austenization temperature (T_{AC3}) the deeper will be the hardened depth, so the ideal process parameters would be those that maintain the background temperature higher than T_{AC3} temperature as long as possible but reducing the peak temperature to avoid melting of the surface. Thus, in order to maximize the depth of the hardened layer, the optimal parameters in laser hardening process with scanning optics should be those that maximize the background temperature but without reaching peak temperatures that can damage the part. By contrast, if the peak temperatures are reduced to prevent damage in the part surface, it is possible not reaching the required background temperature. In the same way, laser hardening with scanning optics is even faster than conventional laser hardening process, so the depth of hardened layer can be lower than a millimeter.

In order to analyze the scanner-based laser hardening process, a structural steel AISI 1045 has been selected because it is a well-known material for surface hardening and it has been characterized in other laser hardening studies [20, 1]. This material is a low alloyed structural steel of 0.45% C which has been tested using a scanning strategy with a scanning line of 10 mm wide. Therefore, as it is shown in Table 1, two types of tests have been performed. The type A tests, with constant scanning speed of 1,000 mm/s and variable feed rates between 40 and 140 mm/min and nominal temperatures between 900 °C and 1,350 °C. Once these tests have been carried out, it has proceeded to a second series of tests. In this series of tests, type B tests, all parameters have been maintained constant except the scanning speed. The scanning speed has ranged between 75 mm/s and 2000 mm/s. Therefore, the analysis of the laser hardening process with scanning optics is based on the combined evaluation of the results of type A and B tests. Special attention has been focused on the influence of the different parameters in the hardness results.

Tab. 1 Table of parameters used during the tests.

	Temperature (°C)	V_F (mm/min)	V_S (mm/s)
Type A	900 - 1,350	40 - 140	1,000
Type B	1,350	60	75 - 2,000



The image shows several laser hardened steel samples. The samples are labeled with parameters: '1045', '110', '120', '130', '140', '150', '160', '170', '180', '190', '200', '210', '220', '230', '240', '250', '260', '270', '280', '290', '300', '310', '320', '330', '340', '350', '360', '370', '380', '390', '400', '410', '420', '430', '440', '450', '460', '470', '480', '490', '500', '510', '520', '530', '540', '550', '560', '570', '580', '590', '600', '610', '620', '630', '640', '650', '660', '670', '680', '690', '700', '710', '720', '730', '740', '750', '760', '770', '780', '790', '800', '810', '820', '830', '840', '850', '860', '870', '880', '890', '900', '910', '920', '930', '940', '950', '960', '970', '980', '990', '1000', '1010', '1020', '1030', '1040', '1050', '1060', '1070', '1080', '1090', '1100', '1110', '1120', '1130', '1140', '1150', '1160', '1170', '1180', '1190', '1200', '1210', '1220', '1230', '1240', '1250', '1260', '1270', '1280', '1290', '1300', '1310', '1320', '1330', '1340', '1350', '1360', '1370', '1380', '1390', '1400', '1410', '1420', '1430', '1440', '1450', '1460', '1470', '1480', '1490', '1500', '1510', '1520', '1530', '1540', '1550', '1560', '1570', '1580', '1590', '1600', '1610', '1620', '1630', '1640', '1650', '1660', '1670', '1680', '1690', '1700', '1710', '1720', '1730', '1740', '1750', '1760', '1770', '1780', '1790', '1800', '1810', '1820', '1830', '1840', '1850', '1860', '1870', '1880', '1890', '1900', '1910', '1920', '1930', '1940', '1950', '1960', '1970', '1980', '1990', '2000', '2010', '2020', '2030', '2040', '2050', '2060', '2070', '2080', '2090', '2100', '2110', '2120', '2130', '2140', '2150', '2160', '2170', '2180', '2190', '2200', '2210', '2220', '2230', '2240', '2250', '2260', '2270', '2280', '2290', '2300', '2310', '2320', '2330', '2340', '2350', '2360', '2370', '2380', '2390', '2400', '2410', '2420', '2430', '2440', '2450', '2460', '2470', '2480', '2490', '2500', '2510', '2520', '2530', '2540', '2550', '2560', '2570', '2580', '2590', '2600', '2610', '2620', '2630', '2640', '2650', '2660', '2670', '2680', '2690', '2700', '2710', '2720', '2730', '2740', '2750', '2760', '2770', '2780', '2790', '2800', '2810', '2820', '2830', '2840', '2850', '2860', '2870', '2880', '2890', '2900', '2910', '2920', '2930', '2940', '2950', '2960', '2970', '2980', '2990', '3000', '3010', '3020', '3030', '3040', '3050', '3060', '3070', '3080', '3090', '3100', '3110', '3120', '3130', '3140', '3150', '3160', '3170', '3180', '3190', '3200', '3210', '3220', '3230', '3240', '3250', '3260', '3270', '3280', '3290', '3300', '3310', '3320', '3330', '3340', '3350', '3360', '3370', '3380', '3390', '3400', '3410', '3420', '3430', '3440', '3450', '3460', '3470', '3480', '3490', '3500', '3510', '3520', '3530', '3540', '3550', '3560', '3570', '3580', '3590', '3600', '3610', '3620', '3630', '3640', '3650', '3660', '3670', '3680', '3690', '3700', '3710', '3720', '3730', '3740', '3750', '3760', '3770', '3780', '3790', '3800', '3810', '3820', '3830', '3840', '3850', '3860', '3870', '3880', '3890', '3900', '3910', '3920', '3930', '3940', '3950', '3960', '3970', '3980', '3990', '4000', '4010', '4020', '4030', '4040', '4050', '4060', '4070', '4080', '4090', '4100', '4110', '4120', '4130', '4140', '4150', '4160', '4170', '4180', '4190', '4200', '4210', '4220', '4230', '4240', '4250', '4260', '4270', '4280', '4290', '4300', '4310', '4320', '4330', '4340', '4350', '4360', '4370', '4380', '4390', '4400', '4410', '4420', '4430', '4440', '4450', '4460', '4470', '4480', '4490', '4500', '4510', '4520', '4530', '4540', '4550', '4560', '4570', '4580', '4590', '4600', '4610', '4620', '4630', '4640', '4650', '4660', '4670', '4680', '4690', '4700', '4710', '4720', '4730', '4740', '4750', '4760', '4770', '4780', '4790', '4800', '4810', '4820', '4830', '4840', '4850', '4860', '4870', '4880', '4890', '4900', '4910', '4920', '4930', '4940', '4950', '4960', '4970', '4980', '4990', '5000', '5010', '5020', '5030', '5040', '5050', '5060', '5070', '5080', '5090', '5100', '5110', '5120', '5130', '5140', '5150', '5160', '5170', '5180', '5190', '5200', '5210', '5220', '5230', '5240', '5250', '5260', '5270', '5280', '5290', '5300', '5310', '5320', '5330', '5340', '5350', '5360', '5370', '5380', '5390', '5400', '5410', '5420', '5430', '5440', '5450', '5460', '5470', '5480', '5490', '5500', '5510', '5520', '5530', '5540', '5550', '5560', '5570', '5580', '5590', '5600', '5610', '5620', '5630', '5640', '5650', '5660', '5670', '5680', '5690', '5700', '5710', '5720', '5730', '5740', '5750', '5760', '5770', '5780', '5790', '5800', '5810', '5820', '5830', '5840', '5850', '5860', '5870', '5880', '5890', '5900', '5910', '5920', '5930', '5940', '5950', '5960', '5970', '5980', '5990', '6000', '6010', '6020', '6030', '6040', '6050', '6060', '6070', '6080', '6090', '6100', '6110', '6120', '6130', '6140', '6150', '6160', '6170', '6180', '6190', '6200', '6210', '6220', '6230', '6240', '6250', '6260', '6270', '6280', '6290', '6300', '6310', '6320', '6330', '6340', '6350', '6360', '6370', '6380', '6390', '6400', '6410', '6420', '6430', '6440', '6450', '6460', '6470', '6480', '6490', '6500', '6510', '6520', '6530', '6540', '6550', '6560', '6570', '6580', '6590', '6600', '6610', '6620', '6630', '6640', '6650', '6660', '6670', '6680', '6690', '6700', '6710', '6720', '6730', '6740', '6750', '6760', '6770', '6780', '6790', '6800', '6810', '6820', '6830', '6840', '6850', '6860', '6870', '6880', '6890', '6900', '6910', '6920', '6930', '6940', '6950', '6960', '6970', '6980', '6990', '7000', '7010', '7020', '7030', '7040', '7050', '7060', '7070', '7080', '7090', '7100', '7110', '7120', '7130', '7140', '7150', '7160', '7170', '7180', '7190', '7200', '7210', '7220', '7230', '7240', '7250', '7260', '7270', '7280', '7290', '7300', '7310', '7320', '7330', '7340', '7350', '7360', '7370', '7380', '7390', '7400', '7410', '7420', '7430', '7440', '7450', '7460', '7470', '7480', '7490', '7500', '7510', '7520', '7530', '7540', '7550', '7560', '7570', '7580', '7590', '7600', '7610', '7620', '7630', '7640', '7650', '7660', '7670', '7680', '7690', '7700', '7710', '7720', '7730', '7740', '7750', '7760', '7770', '7780', '7790', '7800', '7810', '7820', '7830', '7840', '7850', '7860', '7870', '7880', '7890', '7900', '7910', '7920', '7930', '7940', '7950', '7960', '7970', '7980', '7990', '8000', '8010', '8020', '8030', '8040', '8050', '8060', '8070', '8080', '8090', '8100', '8110', '8120', '8130', '8140', '8150', '8160', '8170', '8180', '8190', '8200', '8210', '8220', '8230', '8240', '8250', '8260', '8270', '8280', '8290', '8300', '8310', '8320', '8330', '8340', '8350', '8360', '8370', '8380', '8390', '8400', '8410', '8420', '8430', '8440', '8450', '8460', '8470', '8480', '8490', '8500', '8510', '8520', '8530', '8540', '8550', '8560', '8570', '8580', '8590', '8600', '8610', '8620', '8630', '8640', '8650', '8660', '8670', '8680', '8690', '8700', '8710', '8720', '8730', '8740', '8750', '8760', '8770', '8780', '8790', '8800', '8810', '8820', '8830', '8840', '8850', '8860', '8870', '8880', '8890', '8900', '8910', '8920', '8930', '8940', '8950', '8960', '8970', '8980', '8990', '9000', '9010', '9020', '9030', '9040', '9050', '9060', '9070', '9080', '9090', '9100', '9110', '9120', '9130', '9140', '9150', '9160', '9170', '9180', '9190', '9200', '9210', '9220', '9230', '9240', '9250', '9260', '9270', '9280', '9290', '9300', '9310', '9320', '9330', '9340', '9350', '9360', '9370', '9380', '9390', '9400', '9410', '9420', '9430', '9440', '9450', '9460', '9470', '9480', '9490', '9500', '9510', '9520', '9530', '9540', '9550', '9560', '9570', '9580', '9590', '9600', '9610', '9620', '9630', '9640', '9650', '9660', '9670', '9680', '9690', '9700', '9710', '9720', '9730', '9740', '9750', '9760', '9770', '9780', '9790', '9800', '9810', '9820', '9830', '9840', '9850', '9860', '9870', '9880', '9890', '9900', '9910', '9920', '9930', '9940', '9950', '9960', '9970', '9980', '9990', '10000', '10010', '10020', '10030', '10040', '10050', '10060', '10070', '10080', '10090', '10100', '10110', '10120', '10130', '10140', '10150', '10160', '10170', '10180', '10190', '10200', '10210', '10220', '10230', '10240', '10250', '10260', '10270', '10280', '10290', '10300', '10310', '10320', '10330', '10340', '10350', '10360', '10370', '10380', '10390', '10400', '10410', '10420', '10430', '10440', '10450', '10460', '10470', '10480', '10490', '10500', '10510', '10520', '10530', '10540', '10550', '10560', '10570', '10580', '10590', '10600', '10610', '10620', '10630', '10640', '10650', '10660', '10670', '10680', '10690', '10700', '10710', '10720', '10730', '10740', '10750', '10760', '10770', '10780', '10790', '10800', '10810', '10820', '10830', '10840', '10850', '10860', '10870', '10880', '10890', '10900', '10910', '10920', '10930', '10940', '10950', '10960', '10970', '10980', '10990', '11000', '11010', '11020', '11030', '11040', '11050', '11060', '11070', '11080', '11090', '11100', '11110', '11120', '11130', '11140', '11150', '11160', '11170', '11180', '11190', '11200', '11210', '11220', '11230', '11240', '11250', '11260', '11270', '11280', '11290', '11300', '11310', '11320', '11330', '11340', '11350', '11360', '11370', '11380', '11390', '11400', '11410', '11420', '11430', '11440', '11450', '11460', '11470', '11480', '11490', '11500', '11510', '11520', '11530', '11540', '11550', '11560', '11570', '11580', '11590', '11600', '11610', '11620', '11630', '11640', '11650', '11660', '11670', '11680', '11690', '11700', '11710', '11720', '11730', '11740', '11750', '11760', '11770', '11780', '11790', '11800', '11810', '11820', '11830', '11840', '11850', '11860', '11870', '11880', '11890', '11900', '11910', '11920', '11930', '11940', '11950', '11960', '11970', '11980', '11990', '12000', '12010', '12020', '12030', '12040', '12050', '12060', '12070', '12080', '12090', '12100', '12110', '12120', '12130', '12140', '12150', '12160', '12170', '12180', '12190', '12200', '12210', '12220', '12230', '12240', '12250', '12260', '12270', '12280', '12290', '12300', '12310', '12320', '12330', '12340', '12350', '12360', '12370', '12380', '12390', '12400', '12410', '12420', '12430', '12440', '12450', '12460', '12470', '12480', '12490', '12500', '12510', '12520', '12530', '12540', '12550', '12560', '12570', '12580', '12590', '12600', '12610', '12620', '12630', '12640', '12650', '12660', '12670', '12680', '12690', '12700', '12710', '12720', '12730', '12740', '12750', '12760', '12770', '12780', '12790', '12800', '12810', '12820', '12830', '12840', '12850', '12860', '12870', '12880', '12890', '12900', '12910', '12920', '12930', '12940', '12950', '12960', '12970', '12980', '12990', '13000', '13010', '13020', '13030', '13040', '13050', '13060', '13070', '13080', '13090', '13100', '13110', '13120', '13130', '13140', '13150', '13160', '13170', '13180', '13190', '13200', '13210', '13220', '13230', '13240', '13250', '13260', '13270', '13280', '13290', '13300', '13310', '13320', '13330', '13340', '13350', '13360', '13370', '13380', '13390', '13400', '13410', '13420', '13430', '13440', '13450', '13460', '13470', '13480', '13490', '13500', '13510', '13520', '13530', '13540', '13550', '13560', '13570', '13580', '13590', '13600', '13610', '13620', '13630', '13640', '13650', '13660', '13670', '13680', '13690', '13700', '13710', '13720', '13730', '13740', '13750', '13760', '13770', '13780', '13790', '13800', '13810', '13820', '13830', '13840', '13850', '13860', '13870', '13880', '13890', '13900', '13910', '13920', '13930', '13940', '13950', '13960', '13970', '13980', '13990', '14000', '14010', '14020', '14030', '14040', '14050', '14060', '14070', '14080', '14090', '14100', '14110', '14120', '14130', '14140', '14150', '14160', '14170', '14180', '14190', '14200', '14210', '14220', '14230', '14240', '14250', '14260', '14270', '14280', '14290', '14300', '14310', '14320', '14330', '14340', '14350', '14360', '14370', '14380', '14390', '14400', '14410', '14420', '14430', '14440', '14450', '14460', '14470', '14480', '14490', '14500', '14510', '14520', '14530', '14540', '14550', '14560', '14570', '14580', '14590', '14600', '14610', '14620', '14630', '14640', '14650', '14660', '14670', '14680', '14690', '14700', '14710', '14720', '14730', '14740', '14750', '14760', '14770', '14780', '14790', '14800', '14810', '14820', '14830', '14840', '14850', '14860', '14870', '14880', '14890', '14900', '14910', '14920', '14930', '14940', '14950', '14960', '14970', '14980', '14990', '15000', '15010', '15020', '15030', '15040', '15050', '15060', '15070', '15080', '15090', '15100', '15110', '15120', '15130', '15140', '15150', '15160', '15170', '15180', '15190', '15200', '15210', '15220', '15230', '15240', '15250', '15260', '15270', '15280', '15290', '15300', '15310', '15320', '15330', '15340', '15350', '15360', '15370', '15380', '15390', '15400', '15410', '15420', '15430', '15440', '15450', '15460', '15470', '15480', '15490', '15500', '15510', '15520', '15530', '15540', '15550', '15560', '15570', '15580', '15590', '15600', '15610', '15620', '15630', '15640', '15650', '15660', '15670', '15680', '15690', '15700', '15710', '15720', '15730', '15740', '15750', '15760', '15770', '15780', '15790', '15800', '15810', '15820', '15830', '15840', '15850', '15860', '15870', '15880', '15890', '15900', '15910', '15920', '15930', '15940', '15950', '15960', '15970', '15980', '15990', '16000', '16010', '16020', '16030', '16040', '16050', '16060', '16070', '16080', '16090', '16100', '16110', '16120', '16130', '16140', '16150', '16160', '16170', '16180', '16190', '16200', '16210', '16220', '16230', '16240', '16250', '16260', '16270', '16280', '16290', '16300', '16310', '16320', '16330', '16340', '16350', '16360', '16370', '16380', '16390', '16400', '16410', '16420', '16430', '16440', '16450', '16460', '16470', '16480', '16490', '16500', '16510', '16520', '16530', '16540', '16550', '16560', '16570', '16580', '16590', '16600', '16610', '16620', '16630', '16640', '16650', '16660', '16670', '16680', '16690', '16700', '16710', '16720', '16730', '16740', '16750', '16760', '16770', '16780', '16790', '16800', '16810', '16820', '16830', '16840', '16850', '16860', '16870', '16880', '16890', '16900', '16910', '16920', '16930', '16940', '16950', '16960', '16970', '16980', '16990', '17000', '17010', '17020', '17030', '17040', '17050', '17060', '17070', '17080', '17090', '17100', '17110', '17120', '17130', '17140', '17150', '17160', '17170', '17180', '17190', '17200', '17210', '17220', '17230', '17240', '17250', '17260', '17270', '17280', '17290', '17300', '17310', '17320', '17330', '17340', '17350', '17360', '17370', '17380', '17390', '17400', '17410', '17420', '17430', '17440', '17450', '1746

3. Experimental tests procedure and results

3.1 Type A tests: Constant scanning speed tests

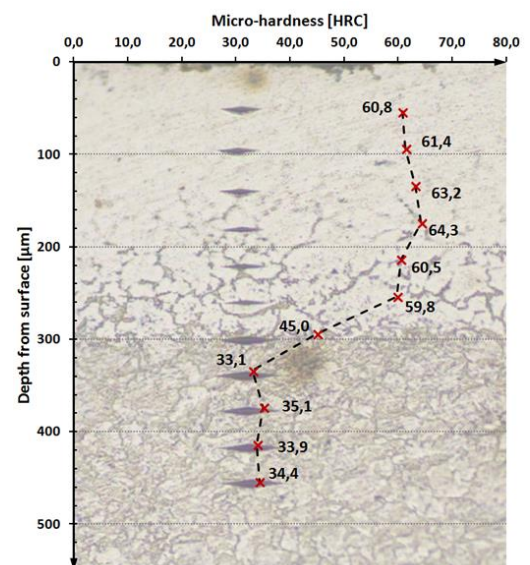
First, a series of tests with constant scanning speed have been performed. The tested parameters and the main results are shown in Table 2. As it can be observed, three nominal temperatures have been tested: 900°C, 1,050°C, 1,200°C and 1,350°C. Results of Table 2 show that a temperature of 900°C is not enough to harden the material.

One relevant conclusion is that the treated area presents a uniform hardness values across all the treated area. This uniformity has been found in all the tests where the treatment has been completed, regardless the nominal temperature values. Analyzing results of conventional laser hardening, in bibliography, it can be observed that the overlap of paths produces three different zones [15], a re-hardened zone, a tempering zone and finally a high temperature tempering zone, usually undesirable for causing an excessive softening of the material. However, it has been observed that this overlapping effect with scanning optics, when the area is scanned at very high speed, do not present any softening zone due to zig-zag strategy effect because the material has not time to cool enough between successive overlaps and it is kept above the martensite formation temperature all the time. In addition, there is not high temperature tempering effect because the hardening is not completed until the area has not been fully scanned.

The micro-hardness measurements performed in the different tests can conclude that the initial hardness in the base material is 33 HRC, obtaining a hardened surface with an average hardness of 63 HRC in the tests where the austenization has been completed. The tests with a nominal temperature of 1,050 °C show a hardness increment with respect the raw material, although it is not as high as it was expected. This effect is because the ratio time-temperature above T_{AC3} is not enough and the material austenization has not been completed. In order to achieve the levels of hardness of the conventional hardening process the nominal temperature should be increased and/or the scanning speed should be decreased.

Tab. 2 Tests results with a constant scanning speed of 1,000 mm/s.

Temperature (°C)	V _F (mm/min)	V _S (mm/s)	Hardened layer (µm)	Hardness (HRC, 500 g)
900	40		-	32.0
900	90		-	32.3
900	140		-	33.9
1,050	40	1,000	185	59.4
1,050	90		125	57.3
1,050	140		110	53.1
1,200	40		385	63.2
1,200	90		260	62.7
1,200	140		230	64.0
1,350	40		580	57.5
1,350	90		365	63.3
1,350	140		300	63.2



As it was expected, the hardened layer thicknesses are deeper if the nominal temperature is increased and the feed rate V_F is decreased, as it is shown in Fig. 4a. Furthermore, evaluating the laser power of the tests versus the nominal temperature (Fig. 4b), it can be concluded that higher laser power is required to increase the temperature 150 degrees from a temperature of 900 °C than from 1,050 °C. In other words, it can be ensured that in the temperature range of 900 °C - 1,050 °C the phase transformation in solid state occurs and the phase transformation enthalpy is the source of the extra laser power required by the process. Moreover, the experimental data show that nominal temperature 900 °C tests do not achieve any surface hardening, regardless the tested feed rates and scanning speeds, whereas tests between 1,050 °C and 1,350 °C obtain hardened layers for different process speeds.

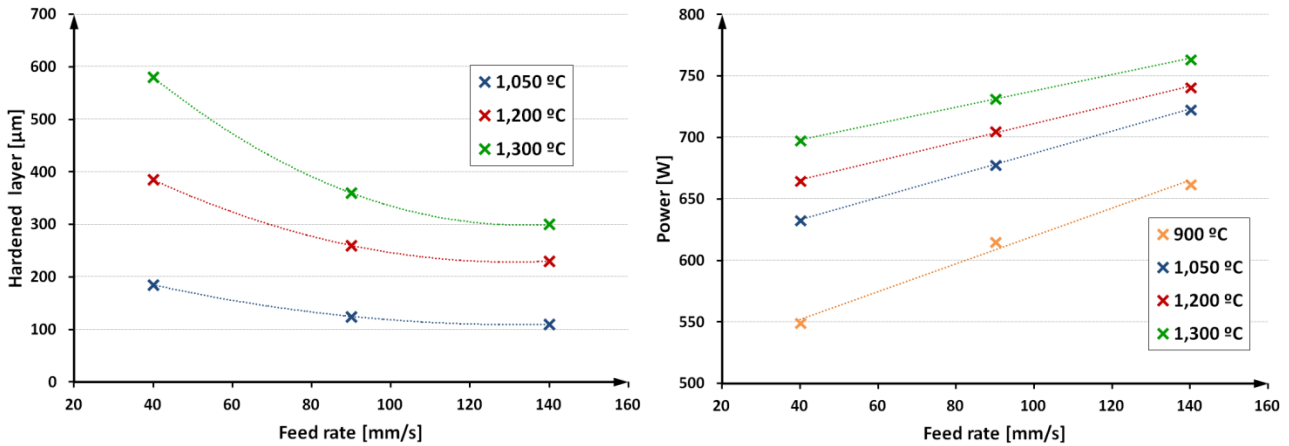


Fig. 4 a) Variation of the hardened depth with the feed rate; **b)** Variation of the average power with the feed rate

3.2 Tests type B: Tests with different scanning speeds

Once the first tests have been carried out, a second group of tests have been performed. The purpose of these tests is to observe the influence of the variation of the scanning speed in the shape of the hardened layer. Therefore, the feed rate and the nominal temperature have been maintained constant, varying only the scanning speed. The nominal temperature has been set to 1,350 °C and the feed rate (V_F) to 60 mm/min, since best results were obtained in the previous tests. The tested parameters and the depth of the hardened layer are shown in Table 3. As expected, tests results show a hardened layer depth below 0.6 mm, far from hardened depths of other treatment processes. Moreover, this fact is aggravated by the laser power used, which is limited to 1 kW. A deeper hardened layer would be expected with higher power equipment.

A deeper analysis of these tests shows two different process regimes that depend on the scanning speed. Thus, if the hardened layer is analyzed in a transversal section, it can be observed that present two different shapes. The first one appears at low scanning speeds, and presents an almost constant thickness but with the maximum hardened thickness near the side limits. By contrast, at high scanning speeds the hardened layer shape is similar to the one which appears in conventional laser hardening process, with a semi-elliptical shape with the maximum hardened thickness in the center of the hardened track. This effect and the difference between zones are shown in the Fig. 5.

Consequently with the obtained results, it can be concluded that the programmed parameters to scan a determined area have a significant effect on the process, due to the variation of the thermal field and, therefore, the cycle of heating – cooling that occurs during the process at each point. The Fig. 5 shows the effect of a variable scanning speed on different temperature measurements during the process. These measurements are always done in the same point on the surface of the part, located at the center of the hardened area. At low scanning speeds, since the feed rate is maintained, there is a larger separation between consecutive lines of the laser beam. In these conditions, the hardening occurs when the peaks temperature exceeds T_{AC3} , even if the background temperature does not reach this value. This is because at low scanning speeds (below 500 mm/s), the laser heats longer and temperatures above T_{AC3} at deeper levels are reached, resulting on a higher thickness of the hardened area. However, an increment of the scanning speed, keeping constant the rest of

parameters, shows that the background temperature increases while the variation peak-background temperature is so fast that this effect is not nearly observed. If the background temperature exceeds T_{AC3} , maintaining a fast scanning speed the deepest hardened thicknesses are obtained.

Tab. 3 Tests results with a variable scanning speed.

Temperature (°C)	V_F (mm/min)	V_S (mm/s)	Hardened layer (μm)
1,350	60	75	335
		125	270
		250	172
		333	135
		500	114
		750	348
		1,000	491
		1,500	525
		2,000	538

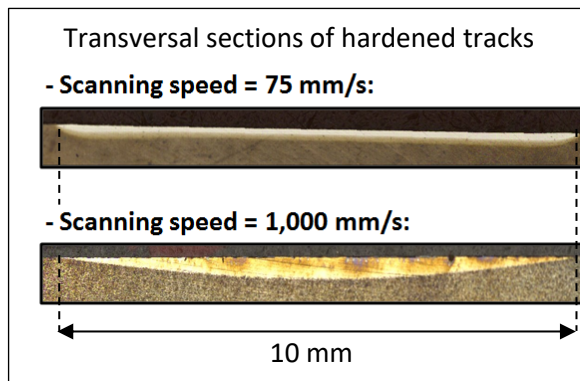
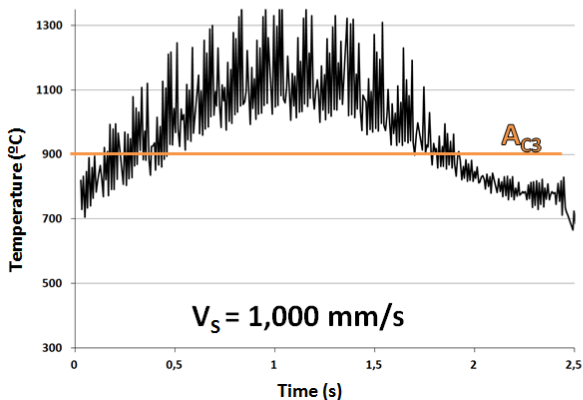
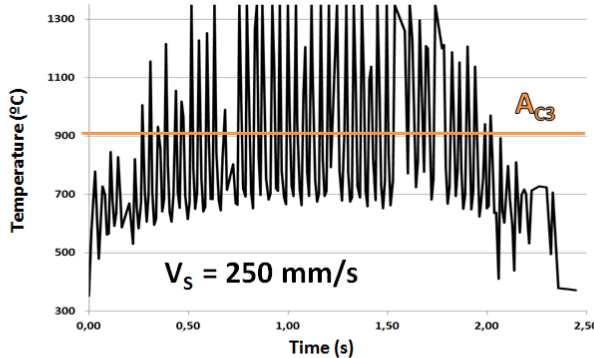
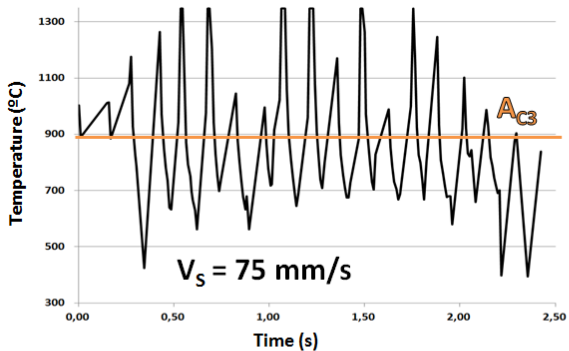
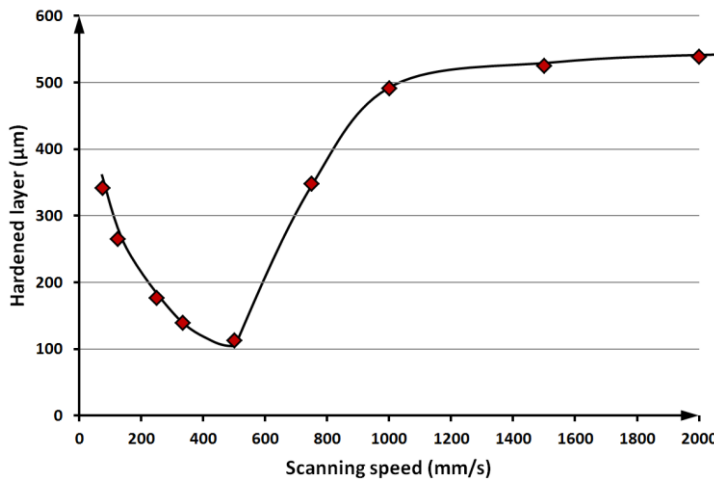


Fig. 5 Measured temperature at the center of the hardened track and shape of the hardened depth with different scanning speeds.

4. Results discussion by means of thermal simulations

Since the laser beam sweeps the treated surface, the temperature ripple during scanner-based laser hardening process is inevitable and intrinsic to the process. In order to understand the resulting thermal field in the part, a deeper analysis of the temperature gradients shows two different process regimens depending on the scanning speed, maintaining the same feed rate [19]. In order to analyze the process regimes more deeply, the Temperature - Time - Position evolution in different zones of the scanned tracks has been obtained by means of simulation of the temperature field. As it is shown in Fig. 6, at low scanning speeds temperature peaks at the trackside are higher than the central point and the temperature ripples are much more significant. If the scanning speed is increased, the simulation shows that the maximum peak of temperature is at the center of the track. Moreover, the temperature signal is smoother while the ripples are attenuated.

These simulations and regime definition is coherent with the two different shapes of the hardened layer, as it has been previously shown in Fig. 5 where Type B tests results are shown. The first one, the rippled state shown in Fig. 6a), can be found at low scanning speeds, and presents an almost constant thickness but with the maximum hardened thickness near the side limits. By contrast, the continuous regime shown in Fig. 6b), is achieved at high scanning speeds and presents a hardened layer shape similar to the conventional laser hardening process, with a semi-elliptical shape with the maximum hardened thickness in the center of the line, coherent with a smoother temperature value.

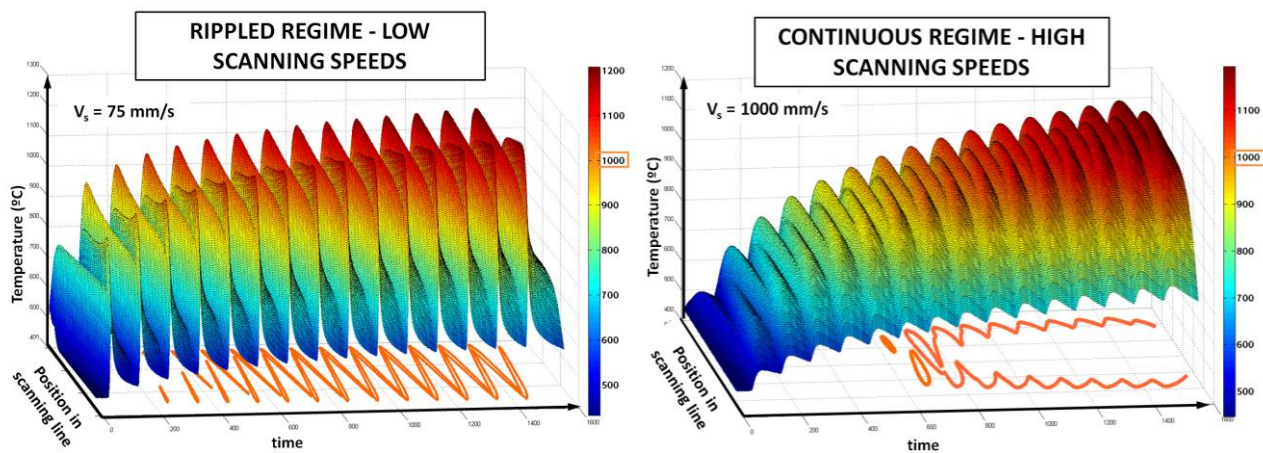


Fig. 6 a) Temperature-time-position in the rippled regime; b) Temperature-time-position in the continuous regime.

Continuous regime can be explained by conventional laser hardening process regime, but rippled regime present higher complexity. Thus, in order to analyze the rippled regime more deeply, the Temperature - Time graphs in different positions of the track has been obtained. Figure 7 shows the evolution of the temperature at 3 different points. First, point A, is located at the central line of the track, point B is near the limit of the track and point C is at the trackside. As it can be observed, temperature of the point A presents temperature peaks ranging $1,350^\circ\text{C}$ (nominal value of the temperature set at the PID control), while temperature at point C exceeds $1,400^\circ\text{C}$. However, the background temperature at point A is higher than point C (about 500°C versus 350°C). This phenomenon is due to the frequency difference of the laser scanning at each point. At the tracksides, the laser only passes once, while the center point (point A) passes twice. On the other hand, the laser at the limits needs to slowdown, invert the motion and accelerate, so the laser beam is present more time. The result is that peak temperature at the tracksides is higher than the central point but the time lapse is longer, so the maximum hardened depth is not achieved at the sides of the track but at the center. As a result of this study, it can be concluded that the analysis of the areas where the maximum background temperature will be achieved is a key factor for the positioning of the pyrometer in order to control the process. Therefore, for high scanning speeds (higher than 750 mm/s) or continuous regime, it is shown that the optimum point for positioning the pyrometer is the center of the track, whereas for low scanning speeds (lower than 200 mm/s) or rippled regimen it is recommended to measure the temperature near one of the tracksides [19].

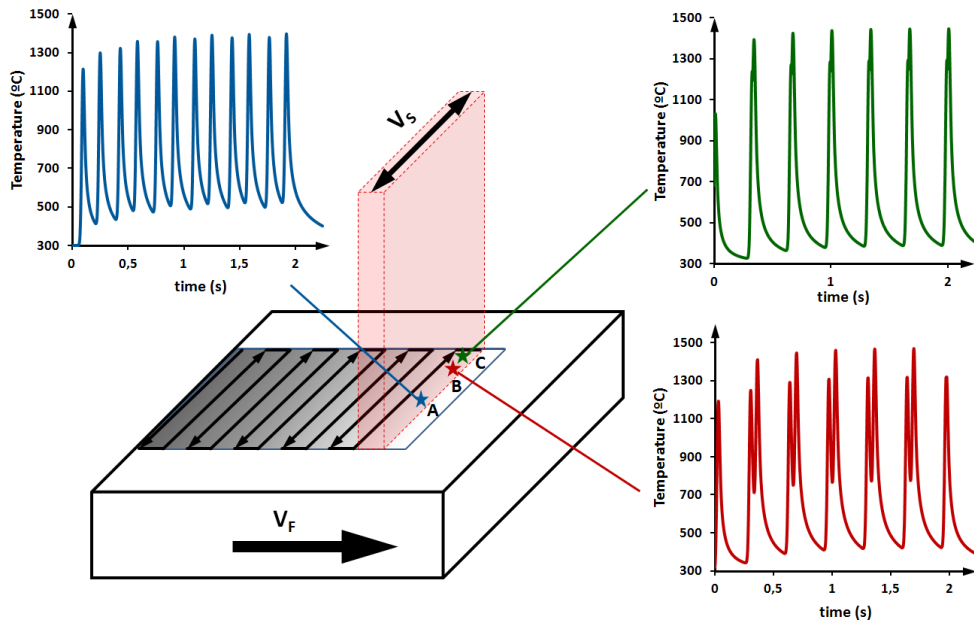


Fig. 7 Measured temperature (measured by a two color pyrometer) in different points of the hardened track with scanning speed=75 mm/s.

Finally, in order to differentiate the rippled and continuous regimes, a series of simulations for different scanning speeds and nominal temperatures were performed. In Fig 8, the result of the simulation shows the different ranges where continuous and rippled regimes are present. As it can be observed, higher scanning speeds and higher nominal temperature values favour the continuous regime, while lower scanning speeds and nominal temperature values result on rippled regime.

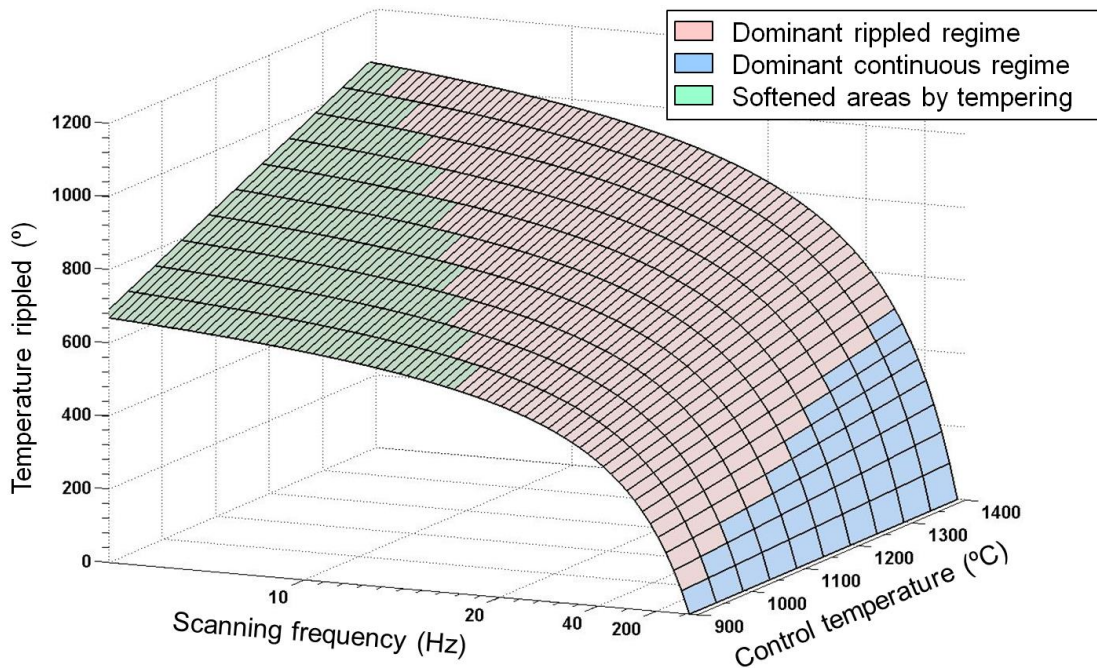


Fig. 8 Regime identification as a function of the nominal temperature and cooling rate between scans

5. Conclusions

Scanner-based laser hardening process presents an inherent variation of the temperature due to the scan effect of the laser beam. Main effects of this process are the thinner hardened layer and the difficulty of controlling the temperature, since it depends on the position at which the pyrometer is focused. The temperature measurements show a background

temperature in combination with temperature peaks. While the background temperature must be necessarily higher than temperature T_{AC3} to increase the hardened area, peaks temperatures should never exceed melting temperature. A deeper study of the process based on the experimental results is summarized below:

- It is possible to obtain conventional hardness values on the surface using the laser scanner-based hardening process. In this case the hardened layer thickness is always lower than 600 μm , because of the laser power is limited to 1 KW. On the other hand, the energy density radiated to the material is lower and it is more localized.
- The flexibility of the process is highly increased since the treated area is scanned with a smaller laser beam, and it is possible to change the scanning strategy, the beam power and scanning speed at each position of the area to be treated. In addition, it is possible to use the same laser machine and accessories for other type of laser processes such as marking, texturing or welding.
- The most relevant parameter in the hardened layer depth is the scanning speed. Also it has influence on the shape of the hardened layer. The maximum thickness of hardened material is obtained at higher scanning speeds when the background temperature exceeds the austenitization temperature of the material.
- Depending on the scanning speed, two different process regimes have been detected. If the scanning speed is higher than 750 mm/s and nominal temperature is set higher than 1,150 $^{\circ}\text{C}$ the temperature field is relatively smooth and hardened track is similar to conventional laser hardened tracks. On the other hand, if the scanning speed drops below 200mm/s, temperature field present a rippled shape and the shape of the hardened track present deeper treated areas at the tracksides.
- The in-process control of the temperature during the scanner-based laser hardening process present more difficulties than in conventional laser hardening process, since the maximum temperature area depends on the process regime. Therefore, process parameters such as the scanning speed or the hardened track width. Moreover, the maximum temperature point position also depends on the regime. In addition, the control – loop has to be significantly faster than in conventional laser hardening process.

Acknowledgments

Special thanks are addressed to the Industry and Competitiveness Spanish Ministry for the support on the DPI2013-46164-C2-1-R TURBO project. Thanks to La Caixa foundation for its financial help.

References

- [1] R. Poprawe. *Tailored Light 2 - Laser Application Technology*. Springer; 2011.
- [2] H. K. D. H. Bhadeshia. *Steels for bearings*. Progress in Materials Science 2012; 57: 268-437.
- [3] F. E. Pfefferkorn, N. A. Duffie, X. Li, M. Vadali, C. Ma. *Improving surface finish in pulsed laser micro polishing using thermocapillary flow*. CIRP Annals - Manufacturing Technology 2013; 62: 203-206.
- [4] K. Kim, K. Yoon, J. Suh, J. Lee. *Laser Scanner Stage On-The-Fly Method for ultrafast and wide Area Fabrication*. Physics Procedia 2011; 12: 452-458.
- [5] J. Diaci, D. Bracun, A. Gorkic, J. Mozina. *Rapid and flexible laser marking and engraving of tilted and curved surfaces*. Optics and lasers in engineering 2011; 49:195-199.
- [6] G. Reinhart, U. Munzert, W. Vogl. *A programming system for robot-based remote-laser-welding with conventional optics*. CIRP Annals - Manufacturing Technology 2008; 57: 37-40.
- [7] I. Arrizubieta, A. Lamikiz, S. Martínez, E. Ukar, I. Tabernero, F. Girot, *Internal characterization and hole formation mechanism in the laser percussion drilling process*, Int. J. of Machine Tools and Manufacture 2013; 75: 55-62.
- [8] D. Dai, D. Gu, *Influence of thermodynamics within molten pool on migration and distribution state of reinforcement during selective laser melting of AlN/AlSi10Mg composites*. Int. J. of Machine Tools and Manufacture 2016; 100: 14-24.
- [9] C. Brecher, M. Emonts, M. Eckert, M. Weinbach, *Double sided irradiation for laser-assisted shearing of ultra-high strength steels with process integrated hardening*. Physic Procedia 2014; 56:1427-1435.
- [10] J. Bliedner, A. Barz, K. Hecht, A. M. Schwager, *Investigations on Laser Forming of Flat Glasses*. Procedia Engineering 2015; 100: 314-320.

- [11] F. Klocke, C. Brecher, D. Heinen, C.J. Rosen, T. Breitbach. *Flexible scanner-based laser surface treatment*. Physics Procedia 2010; 5: 467-475.
- [12] G. H. Farrahi, M. Sistaninia. *Thermal Analysis of Laser Hardening for Different Moving Patterns*. IJE Transactions A: Basics2009; 22: 169-180.
- [13] F. Cordovilla, Á. García-Beltrán, P. Sancho, J. Domínguez, L. Ruiz-de-Lara, J. L. Ocaña, *Numerical/experimental analysis of the laser surface hardening with overlapped tracks to design the configuration of the process for Cr-Mo steels*, Materials & Design 2016; 102: 225-237.
- [14] M. K. H. Leung, H.C. Man, J. K. Yu. *Theoretical and experimental studies on laser transformation hardening of steel by customized beam*. International Journal of heat and Mass Transfer 2007; 50: 4600-4606.
- [15] S. Martínez, A. Lamikiz, I. Tabernero, E. Ukar. *Laser Hardening Process with 2D Scanning Optic*. Physics Procedia 2012; 39: 309-317.
- [16] R. S. Lakhkar, Y. C. Shin, M. J. M. Krane. *Predictive modeling of multi-track laser hardening of AISI 4140 steel*. Materials Science and Engineering A 2008; 480: 209-217.
- [17] Y. Chengwu, X. Binshi, H. Jian, Z. Peilei, W. Yixiong. *Study on the softening in overlapping zone by laser-overlapping scanning surface hardening for carbon and alloyed steel*. Optics and Lasers in Engineering 2010; 48: 20-26.
- [18] M.F. Chen, Y.P. Chen. *Compensating technique of field-distorting error for the CO₂ laser galvanometric scanning drilling machines*. Int. J Machine Tools & Manufacture 2007; 47: 1114-1124.
- [19] S. Martinez, A. Lamikiz, E. Ukar, I. Tabernero, I. Arrizubieta. *Control loop tuning by thermal simulation applied to the laser transformation hardening with scanning optics process*. Applied Thermal Engineering 2016; 98: 49-60.
- [20] I. Magnabosco, P. Ferro, A. Tiziani, F. Bonollo, *Induction heat treatment of a ISO C45 steel bar: Experimental and numerical analysis*. Computational Materials Science 2006, 35: 98-106.